CHINESE OPTICS LETTERS

Vol. 21, No. 1 | January 2023

Directly modulated 25 Gbaud/s tunable in-series DFB laser array for WDM systems

Zhenxing Sun (孙振兴)[1], Yaguang Wang (王亚光)[1], Rulei Xiao (肖如磊)[1*], Leilei Wang (王磊磊)[1], Yangyang Gong (龚洋洋)[1], Yi-Jen Chiu (邱逸仁)[2], and Xiangfei Chen (陈向飞)[1**]

[1] Key Laboratory of Intelligent Optical Sensing and Manipulation of the Ministry of Education & Nanjing University-Tongding Joint Lab for Large-scale Photonic Integrated Circuits & National Laboratory of Solid-State Microstructures & College of Engineering and Applied Science & Institute of Optical Communication Engineering, Nanjing University, Nanjing 210093, China

[2] Department of Photonics and Institute of Electro-Optical Engineering, Taiwan Sun Yat-sen University, Kaohsiung 80424, China

*Corresponding author: xrl@nju.edu.cn

**Corresponding author: chenxf@nju.edu.cn

Received May 12, 2022 | Accepted July 22, 2022 | Posted Online September 21, 2022

In this Letter, we proposed and experimentally demonstrated a directly modulated tunable laser based on the multi-wavelength distributed feedback (DFB) laser array. The lasers are placed in series to avoid the usage of an optical combiner and additional power loss. A three-section design is utilized to reduce the interference from other lasers and improve the electro-optic response bandwidth. Besides, the reconstruction-equivalent-chirp technique is used to simplify the grating fabrication and precisely control the grating phase. We realized 12 channels with 100 GHz spacing with high side mode suppression ratios of above 50 dB. The output power of all the channels is above 14 mW. The 3 dB electro-optic bandwidth is above 20 GHz at a bias current of 100 mA for all four lasers. A 25 Gb/s data transmission over a standard single-mode fiber of up to 10 km is demonstrated for all 12 channels, and 50 Gb/s data per wavelength is obtained through the four-level pulse amplitude modulation. The proposed directly modulated tunable in-series DFB laser array shows the potential for a compact and low-cost light source for wavelength division multiplexing (WDM) systems, such as next-generation front-haul networks and passive optical networks.

Keywords: tunable laser; directly modulated laser; laser array; wavelength division multiplexing.
DOI: 10.3788/COL202321.011403

1. Introduction

Wavelength-division-multiplexing (WDM) technology has recently shown great potential in the metro and access networks. WDM networks are expected to be applied in next-generation high-capacity front-haul networks and passive optical networks[1,2]. Wavelength tunable semiconductor lasers are very important components in WDM networks. The lasers with fixed wavelengths are desired to be replaced by tunable lasers for enhancing the network flexibility and reducing the system costs[3,4]. Besides, high-speed modulation per wavelength is required for the increasing data traffic[5]. Tunable lasers with different tuning mechanisms have been investigated and reported, including the tunable distributed Bragg reflector (DBR) lasers, the external-cavity tunable lasers (ECTLs), the Vernier-effect-based tunable lasers, and the multi-wavelength distributed feedback (DFB) laser arrays (MLAs)-based tunable lasers[6–10]. The tunable lasers based on the MLAs are superior for the simple wavelength tuning mechanism and the stable single-mode operations. The conventional multi-wavelength laser arrays are placed in parallel, and an extra optical combiner is monolithically integrated for the one-waveguide light output[11]. The optical power loss is introduced by the optical combiner, and the fabrication process becomes complex for the integration of the passive optical combiner. Thus, the lasers in the multi-wavelength laser arrays are expected to be arranged in series to avoid the use of the optical combiner. However, the single-mode stabilities are deteriorated by the grating crosstalk from the lasers placed in series, and the grating crosstalk becomes quite serious when the wavelength spacing is smaller than the width of the grating stopband, which is typically 3.2 nm in the DFB laser[12]. However, a large temperature range is required to tune the wavelength of interest if the wavelength spacing of the laser arrays is too large. The large temperature tuning range may increase the power consumption of the thermoelectric cooler (TEC), cause a large difference in the laser output power, and accelerate the aging of the device.

Here, we demonstrate a high-speed directly modulated tunable in-series laser array (DMTL) with four integrated lasers, and the Bragg wavelengths of the four lasers are separated by 2.4 nm.

A three-section design is utilized to reduce the interference from other lasers and obtain good single-mode properties. Based on the three-section structure, the electro-optic (EO) response bandwidth can be enhanced owing to the reduced modulated cavity length. Meanwhile, the photon intensity stays high along the modulated section owing to the π phase shift cavity design, which is beneficial to a high resonant frequency. Besides, we utilize the reconstruction-equivalent-chirp (REC) technique to simplify the grating fabrication process and enhance the precise control of the grating phase. Therefore, the proposed DMTL shows the advantages of compact device size and a simple fabrication process. In addition, a semiconductor optical amplifier (SOA) is designed in front of the laser array to amplify the output power.

2. Device Design and Fabrication

2.1. Device design

The key to realizing a high-speed DMTL is to increase the modulation bandwidth and reduce the crosstalk among the gratings of the in-series lasers. The relaxation oscillation frequency (f_r) of the lasers should be increased as high as possible, and the resistor-capacitor (RC) constant should be decreased to meet the high bandwidth requirement[13–15]. The relaxation oscillation frequency can be expressed as follows[16]:

$$f_r = \frac{1}{2\pi}\sqrt{v_g g' S_0/\tau_P}, \tag{1}$$

where v_g is the group velocity, S_0 is the steady-state photon density in the cavity, g' is differential gain, and τ_P is the photon lifetime. Reducing the active region length is an effective method to decrease the photon lifetime and increase the photon density in the cavity, thus improving the relaxation oscillation frequency[17]. However, a short active region length for DFB lasers will reduce the optical feedback of the grating, which results in high threshold gain and finally deteriorates the direct modulation bandwidth. In this Letter, we propose a three-section π phase-shifted directly modulated DFB laser, which includes a short central gain section (GS) and two side sections (SSs), as shown in Fig. 1(a). The simulated distribution of the photon intensity along the cavity is shown in Fig. 1(b). Photons are concentrated in the central GS owing to the π phase shift. Therefore, the central GS is injected with a large current for lasing and modulation. The SSs share the same multiple quantum wells (MQWs) and grating period as the central GS. The SSs are injected with a small current to provide additional feedback. As a result, a low threshold gain of the GS is obtained owing to the additional feedback from the SSs. Moreover, the relaxation oscillation frequency is enhanced owing to the high differential gain and photon density of the GS. The shortened gain length also lowers the parasitic capacitance. A thick benzocyclobutene (BCB) layer is designed underneath the p electrode of the central GS to further decrease the parasitic capacitance.

In addition, the three-section structure can help suppress the side modes to guarantee the single-mode operations. As shown in Fig. 1(b), the photons of the dominant lasing mode in the cavity are mainly distributed around the center of the cavity, which is different from the side modes. Therefore, the priority of the dominant lasing mode can be increased by the different current injections to the central GS and the SSs. Thus, the single-mode stabilities can be enhanced. Besides, a phase error of the grating in the whole cavity may destroy the single-mode properties, and the grating phase precision can be improved through the REC technique. The REC technique studied in previous work uses a sampled grating to introduce equivalent π phase shifts and improve the precision of the grating phase[18–20]. Usually, we use a +1st-order grating to provide grating feedback and select the lasing mode for its high equivalent coupling coefficient and its ability to introduce equivalent π phase shift. The Bragg wavelength of the +1st-order grating (λ_{+1}) is determined by the sampling period (P), and the variation of λ_{+1} is derived as Eq. (2). The λ_{+1} is not sensitive to the variation of the sampling period, and thus the grating fabrication tolerance is relaxed by the factor $(P/\Lambda_0 + 1)^2$, with the value of several hundred. The schematic

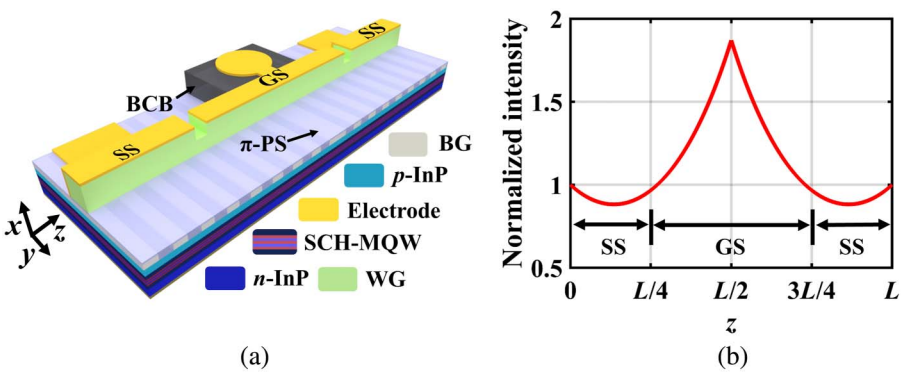

Fig. 1. (a) Schematic of the proposed structure of one laser unit and (b) calculated normalized optical intensity of the lasing mode along the cavity of one laser unit. (SS, side section; GS, gain section; SCH-MQW, separate confinement hetero-structure-multi-quantum well; BG, Bragg grating; BCB, benzocyclobutene; WG, waveguide).

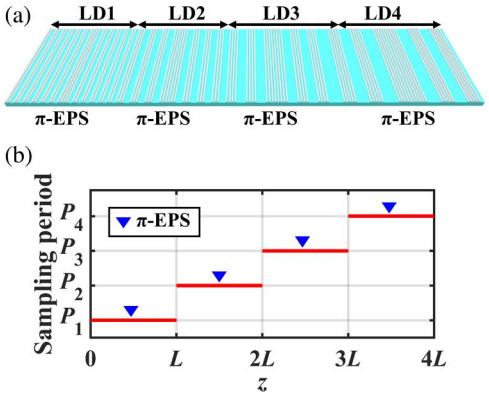

Fig. 2. (a) Schematic of the grating designed by the REC technique and (b) sampling periods of the four in-series lasers (π-EPS: equivalent π phase shift).

of the grating designed based on the REC technique is shown in Fig. 2(a), and the sampling period of the four integrated lasers is shown in Fig. 2(b):

$$\Delta\lambda_{+1} = \frac{1}{\left(\frac{P}{\Lambda_0}+1\right)^2} 2n\Delta P. \tag{2}$$

2.2. Device fabrication

We adopted a standard ridged waveguide structure for the proposed in-series laser array for its simple fabrication process. The compressively-strained InAlGaAs MQW structure is utilized as the active layer for its excellent high-temperature performance. The p-InGaAsP is used as the grating layer. The thickness of the p-InGaAsP grating layer is 50 nm, and the photoluminescence (PL) wavelength of the p-InGaAsP grating layer is 1.36 μm. The coupling coefficient of the uniform grating is approximately 9300 m^{-1} to guarantee that the coupling coefficient of the +1st-order sub-grating is 3000 m^{-1}. Owing to the grating design based on the REC technique, the fabrication of the grating only requires a holographic exposure and micrometer (μm)-level photolithography, avoiding the expensive electron beam lithography. The BCB is fabricated underneath the p electrode of the central GS to decrease the parasitic capacitance, thus improving the direct modulation bandwidth. Figure 3 shows the picture of the DMTL chip under the microscope. The four integrated lasers are all 550 μm long, and the GS is 275 μm long. The electrodes of the SSs are connected to simplify the measurement process. The SOA with 250 μm length is integrated to adjust the output power. The total size of the chip is 2500 μm × 300 μm. Both the front and rear facets are coated with anti-reflection films. The output waveguide of the SOA is tilted 7 deg to further decrease the facet reflection.

3. Device Characterization

The proposed DMTL was bonded onto a high-frequency submount to facilitate device characterization. Figure 4(a) shows the fabricated DMTL chip on the submount (COS). AlN is used as the substrate for its high thermal conductivity. The ground coplanar waveguide (GCPW) structure is used to feed the RF signal. The 40 Ω TaN resistor is fabricated for impedance matching. In addition, the RF signals and bias currents are injected separately from two sides. The bias currents are injected into the lasers directly and do not pass the 40-Ω resistors, which effectively decreases the power consumption. The magnetic beads are bonded on the DC line of the substrate to prevent the RF signals.

The DMTL COS is placed on a copper carrier, and the temperature of the carrier can be adjusted by the TEC. We analyzed the lasing spectra using the optical spectrum analyzer (Yokogawa, AQ6370). The temperature of the TEC is set at 25°C first. The currents injected to the GS, SS, and SOA (I_{GS}, I_{SS}, I_{SOA}) are 80, 30, and 30 mA, respectively. When one laser works, the front sections are injected with a small compensation current (I_{com}) to avoid material absorption of the light, and I_{com} is set at 15 mA here. The optical spectra of the four lasers are shown in Fig. 4(b). The fitting slope with the lasing wavelengths of 2.47 nm represents the average wavelength spacing, which only deviates from the design by 0.07 nm. Besides, the side mode suppression ratios (SMSRs) of the lasing modes of the four lasers are 59.5, 52.8, 53.5, and 54.0 dB, respectively. Thus, precise wavelength spacing and good single-mode operations are obtained for all the four lasers.

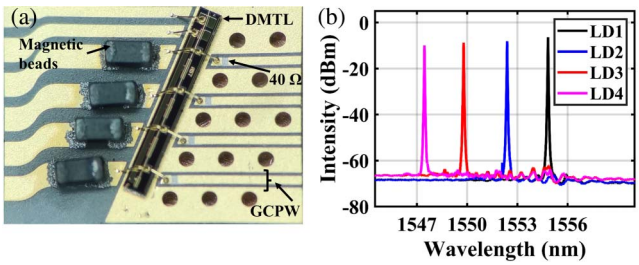

Fig. 4. (a) Microscopic top view of the DMTL COS and (b) superimposed optical spectra of all four lasers (DMTL, directly-modulated tunable in-series laser array; GCPW, ground coplanar waveguide; COS, chip on submount).

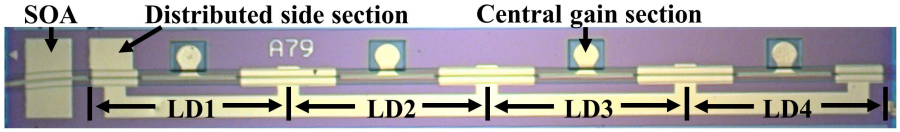

Fig. 3. Picture of the DMTL chip under the microscope (SOA, semiconductor optical amplifier; LD, laser diode).

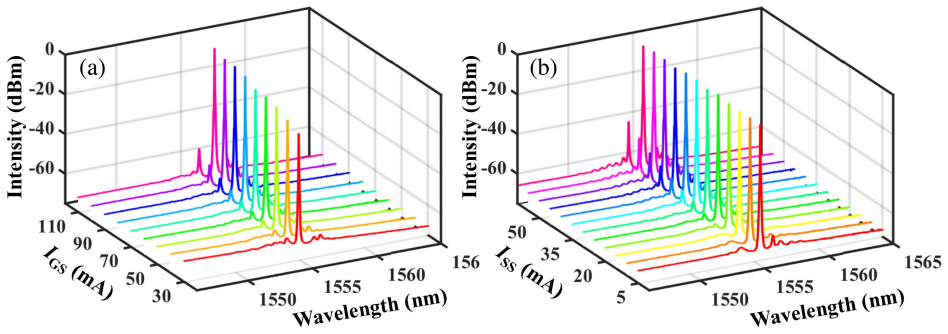

Fig. 5. (a) Optical spectra of LD1 as a function of I_{GS} when I_{SOA} and I_{SS} are both fixed at 30 mA and (b) optical spectra of LD1 as a function of I_{SS} when I_{SOA} and I_{GS} are fixed at 30 and 70 mA, respectively (I_{SOA}, current injected into the semiconductor optical amplifier; I_{GS}, current injected into the gain section; I_{SS}, current injected into the side section).

We studied the impact of I_{GS} and I_{SS} on the lasing performance. We measured the optical spectra of the laser diode (LD1) as an example. As shown in Fig. 5(a), I_{SOA} and I_{SS} are both fixed at 30 mA, and good single-mode operations are kept when I_{GS} is adjusted from 30 to 110 mA. Figure 5(b) shows the optical spectra of LD1 as a function of I_{SS} when I_{SOA} and I_{GS} are fixed at 30 and 70 mA, respectively. The single-mode properties deteriorate when I_{SS} is above 50 mA.

The typical power-current-voltage (*PIV*) curve of LD1 is described in Fig. 6(a). I_{SOA} and I_{SS} are 10 and 30 mA, respectively. Figure 6(a) shows the threshold current is 19 mA, and the differential resistance of the central GS is 12.2 Ω. The performance of the SOA was also characterized. Figure 6(b) shows the output power as a function of I_{SOA}, and the output power of all the lasers can reach 14 mW at I_{SOA} of 60 mA.

The tunable DFB laser arrays are superior for their simple wavelength tuning mechanism. The wavelength of interest can be obtained by selecting the working laser and adjusting the temperature of the TEC. Here, we tuned 12 channels with 100 GHz spacing for our proposed DMTL. I_{GS}, I_{SS}, and I_{com} are 80, 30, and 15 mA, respectively. We adjusted I_{SOA} to keep the output power of all the 12 tuned channels balanced. The optical spectra of the tuned 12 channels with 100 GHz spacing are shown in Fig. 7(a). The temperature variation of the TEC for tuning the 12 channels is only 16°C, which is mainly due to the precise and small wavelength spacing, and the thermal coefficient is approximately 0.11 nm/°C. The right of Fig. 7(b) shows the SMSRs of the tuned 12 channels, and all the SMSRs are above 50 dB, indicating quite good single-mode operations.

The EO response was analyzed using the 70 GHz vector network analyzer (Anritsu MS4647A). The temperature of the TEC is set at 25°C. I_{SOA} and I_{SS} are both 30 mA. Figure 8(a) shows the EO response of LD1 when I_{GS} is different. As is shown in Fig. 8(a), the 3 dB bandwidth is increased at a high I_{GS}. The 3 dB bandwidth reaches 21.3 GHz at the bias current of 100 mA. The EO responses of the four lasers when the I_{GS} is 100 mA are

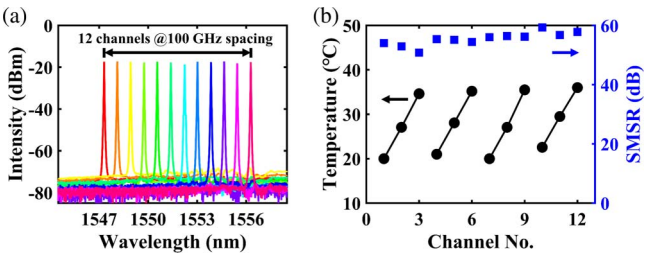

Fig. 7. (a) Lasing spectra of the tuned 12 channels and (b) tuned temperature of the TEC (left) and SMSRs of all the 12 channels (right) (SMSR, side mode suppression ratio).

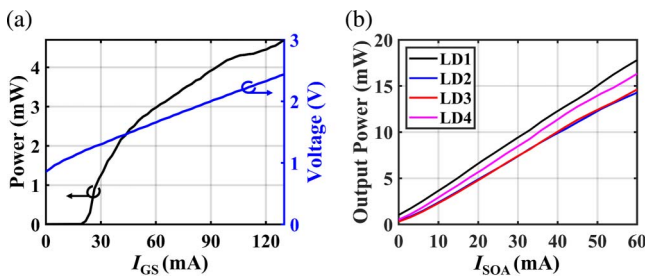

Fig. 6. (a) Power-current-voltage curve of LD1 with I_{SOA} of 10 mA and (b) laser output power as a function of the I_{SOA} for the four lasers with the I_{GS} and I_{SS} set at 80 and 30 mA (I_{SOA}, current injected into the semiconductor optical amplifier; I_{GS}, current injected into the gain section; I_{SS}, current injected into the side section).

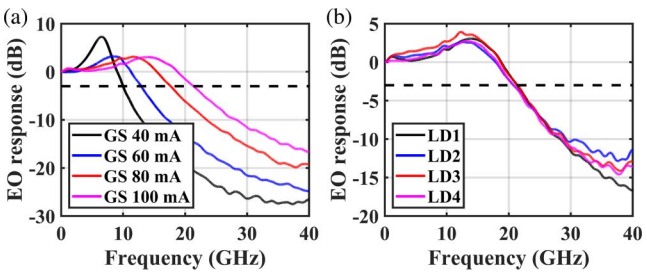

Fig. 8. (a) EO response of LD1 when I_{GS} is varied from 40 to 100 mA and (b) EO response of all the four lasers when I_{GS} is 100 mA (GS, gain section; I_{GS}, current injected into the GS).

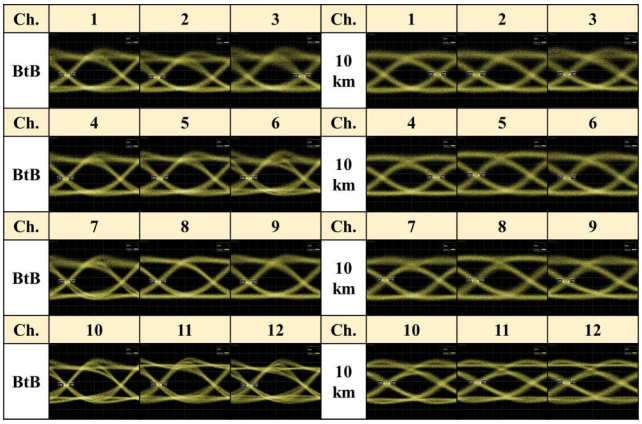

Fig. 9. Measured back-to-back 25 Gb/s NRZ optical eye diagrams and 25 Gb/s NRZ eye diagrams after 10 km transmission for all 12 channels (Ch., channel; BtB, back-to-back).

all analyzed. As shown in Fig. 8(b), the 3 dB bandwidths of the four lasers are 21.3, 20.8, 21.4, and 20.7 GHz, respectively.

The 25 Gb/s non-return-to-zero (NRZ) large-signal modulation was performed with a pseudo-random bit sequence (PRBS) of $2^{31}-1$. The PRBS signal is generated by a 100G bidirectional encoder representation from transformers (BERT, Golight) and amplified by a 38 GHz electrical amplifier (SHF L810A). The peak-to-peak current (I_{PP}) fed to the central GS is about 74 mA. I_{SOA}, I_{SS}, and I_{GS} are 30, 30, and 100 mA, respectively. The optical eye diagrams are analyzed by the optical sampling oscilloscope (Keysight N1092A). The left of Fig. 9 shows the back-to-back optical eye diagrams for all 12 channels. The dynamic extinction ratios of all 12 channels are above 4 dB. The right of Fig. 9 shows the optical eye diagrams of all 12 channels after 10 km transmission over a standard single-mode fiber, and clearly opened eye diagrams are obtained for all 12 channels. Besides, 50 Gb/s data per wavelength can be obtained through the four-level pulse amplitude modulation (PAM4). Figure 10(a) shows the electrical eye digrams of the 50 Gb/s PAM4 signals after the electrical amplifier. Channel 10 is selected as an example to conduct the modulation with the 50 Gb/s PAM4 signals. As shown in Fig. 10(b), a clearly opened PAM4 optical eye diagram is obtained for channel 10.

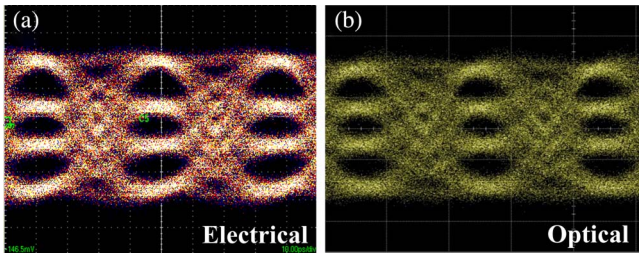

Fig. 10. (a) Electrical eye diagram of the 50 Gb/s PAM4 signal after the electrical amplifier and (b) measured 50 Gb/s PAM4 optical eye diagram for channel 10.

4. Conclusion

In this Letter, we demonstrated a 25 Gbaud/s DMTL. High output power (> 14 mW) and high uniform wavelength spacing are obtained for the proposed tunable in-series laser array. With a temperature variation of only 16°C, 12 channels with 100 GHz spacing are tuned. Good single-mode operations with the SMSRs > 50 dB are obtained for all 12 channels. The 3 dB EO response bandwidth is above 20 GHz for all four lasers at the bias current of 100 mA. NRZ data transmission of 25 Gb/s over a single-mode fiber of up to 10 km is obtained for the proposed device. Besides, 50 Gb/s data per wavelength is obtained through PAM4. The proposed DMTL shows the potential for a compact and low-cost light source for WDM systems, such as next-generation front-haul networks and passive optical networks.

Acknowledgement

This work was supported in part by the Chinese National Key Basic Research Special Fund (Nos. 2017YFA0206401, 2018YFA0704402, 2018YFE0201200, and 2018YFB2201801), National Natural Science Foundation of China (Nos. 62004094 and 61975075), Natural Science Foundation of Jiangsu Province of China (No. BK20200334), Jiangsu Science and Technology Project (Nos. BE2019101 and BE2017003-2), and Suzhou Technological Innovation of Key Industries (No. SYG201844).

References

1. H. Rohde, E. Gottwald, A. Teixeira, J. D. Reis, A. Shahpari, K. Pulverer, and J. S. Wey, "Coherent ultra dense WDM technology for next generation optical metro and access networks," J. Light. Technol. **32**, 2041 (2014).
2. K. Iwatsuki, J. I. Kani, H. Suzuki, and M. Fujiwara, "Access and metro networks based on WDM technologies," J. Light. Technol. **22**, 2623 (2004).
3. J. Buus and E. J. Murphy, "Tunable lasers in optical networks," J. Light. Technol. **24**, 5 (2006).
4. L. A. Coldren, G. A. Fish, Y. Akulova, J. S. Barton, L. Johansson, and C. W. Coldren, "Tunable semiconductor lasers: a tutorial," J. Light. Technol. **22**, 193 (2004).
5. D. Zhou, D. Lu, S. Liang, L. Zhao, and W. Wang, "Transmission of 20 Gb/s PAM-4 signal over 20 km optical fiber using a directly modulated tunable DBR laser," Chin. Opt. Lett. **16**, 091401 (2018).
6. O. K. Kwon, K. H. Kim, E. D. Sim, H. K. Yun, J. H. Kim, H. S. Kim, and K. R. Oh, "Proposal of electrically tunable external-cavity laser diode," IEEE Photon. Technol. Lett. **16**, 1804 (2004).
7. B. Mason, J. Barton, G. A. Fish, L. A. Coldren, and S. P. DenBaars, "Design of sampled grating DBR lasers with integrated semiconductor optical amplifiers," IEEE Photon. Technol. Lett. **12**, 762 (2000).
8. L. Han, S. Liang, C. Zhang, L. Liqiang Yu, L. Zhao, H. Zhu, B. Wang, C. Ji, and W. Wang, "Fabrication of widely tunable ridge waveguide DBR lasers for WDM-PON," Chin. Opt. Lett. **12**, 091402 (2014).
9. B. Pezeshki, E. Vail, J. Kubicky, G. Yoffe, S. Zou, J. Heanue, P. Epp, S. Rishton, D. Ton, B. Faraji, M. Emanuel, X. Hong, M. Sherback, V. Agrawal, C. Chipman, and T. Razazan, "20-mW widely tunable laser module using DFB array and MEMS selection," IEEE Photon. Technol. Lett. **14**, 1457 (2002).

10. J. Hong, H. Kim, F. Shepherd, C. Rogers, B. Baulcomb, and S. Clements, "Matrix-grating strongly gain-coupled (MG-SGC) DFB lasers with 34-nm continuous wavelength tuning range," IEEE Photon. Technol. Lett. **11**, 515 (1999).
11. H. Ishii, K. Kasaya, and H. Oohashi, "Spectral linewidth reduction in widely wavelength tunable DFB laser array," IEEE J. Sel. Top. Quantum Electron. **15**, 514 (2009).
12. L. Li, S. Tang, J. Lu, Y. Shi, B. Cao, and X. Chen, "Study of cascaded tunable DFB semiconductor laser with wide tuning range and high single mode yield based on equivalent phase shift technique," Opt. Commun. **352**, 70 (2015).
13. R.-Y. Chen, Y.-J. Chen, C.-L. Chen, C.-C. Wei, W. Lin, and Y.-J. Chiu, "High-power long-waveguide 1300-nm directly modulated DFB laser for 45-Gb/s NRZ and 50-Gb/s PAM4," IEEE Photon. Technol. Lett. **30**, 2091 (2018).
14. G. Liu, G. Zhao, J. Sun, D. Gao, Q. Lu, and W. Guo, "Experimental demonstration of DFB lasers with active distributed reflector," Opt. Express **26**, 29784 (2018).
15. G. Liu, G. Zhao, G. Zhang, Q. Lu, and W. Guo, "Directly modulated active distributed reflector distributed feedback lasers over wide temperature range operation," Chin. Opt. Lett. **18**, 061401 (2020).
16. R. Nagarajan, M. Ishikawa, T. Fukushima, R. S. Geels, and J. E. Bowers, "High speed quantum-well lasers and carrier transport effects," IEEE J. Quantum Electron. **28**, 1990 (1992).
17. K. Lau and A. Yariv, "Ultra-high speed semiconductor lasers," IEEE J. Quantum Electron. **21**, 121 (1985).
18. Z. Sun, R. Xiao, Z. Su, K. Liu, G. Lv, K. Xu, T. Fang, Y. Shi, Y. J. Chiu, and X. Chen, "Experimental demonstration of wavelength-tunable in-series DFB laser array with 100-GHz spacing," IEEE J. Sel. Top. Quantum Electron. **28**, 1500308 (2022).
19. Y. Shi, X. Chen, Y. Zhou, S. Li, L. Lu, R. Liu, and Y. Feng, "Experimental demonstration of eight-wavelength distributed feedback semiconductor laser array using equivalent phase shift," Opt. Lett. **37**, 3315 (2012).
20. X. Chen, "Precision photonic integration for future large-scale photonic integrated circuits," J. Semicond. **40**, 050301 (2019).